Received: 25 March 2024 | Accepted: 16 May 2024

DOI: 10.1002/bab.2620

ORIGINAL ARTICLE

WILEY

Ohwia caudata inhibits doxorubicin-induced cardiotoxicity by regulating mitochondrial dynamics via the IGF-IIR/p-Drp1/PARP signaling pathway

Jhong-Kuei Chen[1,2,3] | **Samiraj Ramesh**[4,5] | **Md. Nazmul Islam**[4] | **Marthandam Asokan Shibu**[6] | **Chia-Hua Kuo**[7] | **Dennis Jine-Yuan Hsieh**[8,9] | **Shinn-Zong Lin**[10,11] | **Wei-Wen Kuo**[12,13,14] | **Chih-Yang Huang**[4,15,16,17,18] | **Tsung-Jung Ho**[1,2,3,19]

[1]Department of Chinese Medicine, Hualien Tzu Chi Hospital, Buddhist Tzu Chi Medical Foundation, Hualien, Taiwan

[2]Integration Center of Traditional Chinese and Modern Medicine, Hualien Tzu Chi Hospital, Buddhist Tzu Chi Medical Foundation, Hualien, Taiwan

[3]Institute of Medical Sciences, Tzu Chi University, Hualien, Taiwan

[4]Cardiovascular and Mitochondrial Related Disease Research Center, Hualien Tzu Chi Hospital, Buddhist Tzu Chi Medical Foundation, Hualien, Taiwan

[5]Department of Research and Innovation, Institute of Biotechnology, Saveetha School of Engineering (SSE), Saveetha Institute of Medical and Technical Sciences (SIMATS), Chennai, India

[6]Department of Biotechnology, Bharathiar University, Coimbatore, India

[7]Laboratory of Exercise Biochemistry, University of Taipei, Taipei, Taiwan

[8]School of Medical Laboratory and Biotechnology, Chung Shan Medical University, Taichung, Taiwan

[9]Clinical Laboratory, Chung Shan Medical University Hospital, Taichung, Taiwan

[10]Bioinnovation Center, Buddhist Tzu Chi Medical Foundation, Hualien, Taiwan

[11]Department of Neurosurgery, Hualien Tzu Chi Hospital, Buddhist Tzu Chi Medical Foundation, Hualien, Taiwan

[12]Department of Biological Science and Technology, College of Life Sciences, China Medical University, Taichung, Taiwan

[13]Ph.D. Program for Biotechnology Industry, China Medical University, Taichung, Taiwan

[14]School of Pharmacy, China Medical University, Taichung, Taiwan

[15]Graduate Institute of Biomedical Sciences, China Medical University, Taichung, Taiwan

[16]Department of Medical Research, China Medical University Hospital, China Medical University, Taichung, Taiwan

[17]Department of Medical Laboratory Science and Biotechnology, Asia University, Taichung, Taiwan

[18]Center of General Education, Buddhist Tzu Chi Medical Foundation, Tzu Chi University of Science and Technology, Hualien, Taiwan

[19]School of Post-Baccalaureate Chinese Medicine, College of Medicine, Tzu Chi University, Hualien, Taiwan

Correspondence
Chih-Yang Huang, Cardiovascular and Mitochondrial Related Disease Research Center, Hualien Tzu Chi Hospital,

Abstract

The most effective drug, doxorubicin (DOX), is widely used worldwide for clinical application as an anticancer drug. DOX-induced cytotoxicity is characterized

Abbreviations: CVD, cardiovascular disease; DAPI, 4′,6-diamidino-2-phenylindole dihydrochloride; DOX, doxorubicin; Drp1, dynamin-related protein 1; HRP, horseradish peroxidase; IGF-IIR, insulin-like growth factor II receptor; MiD, mitochondrial dynamics proteins; MTT, 3-(4,5-dimethylthiazol-2-yl)–2,5-diphenyltetrazolium-bromide; OC, *Ohwia caudata*; ROS, mitochondrial reactive oxygen species; TBST, Tris-buffered saline Tween-20; TUNEL, terminal deoxynucleotidyl transferase dUTP-mediated nick-end labeling.

Chih-Yang Huang and Tsung-Jung Ho contributed equally to this work.

Buddhist Tzu Chi Medical Foundation, Tzu Chi University of Science and Technology, Hualien 970, Taiwan. Email: cyhuang@mail.cmu.edu.tw

Tsung-Jung Ho, Department of Chinese Medicine, Hualien Tzu Chi Hospital, Buddhist Tzu Chi Medical Foundation, Hualien, Taiwan. Email: jeron888@gmail.com

Funding information
Hualien Tzu Chi Hospital, Buddhist Tzu Chi Medical Foundation, Grant/Award Numbers: IMAR-109-01-04-01, IMAR-112-01-02

by mitochondrial dysfunction. There is no alternative treatment against DOX-induced cardiac damage despite intensive research in the present decades. *Ohwia caudata* has emerged as a potential herbal remedy that prevents from DOX-induced cytotoxicity owing to its pharmacological action of sustaining mitochondrial dynamics by attenuating oxidative stress and inducing cellular longevity. However, its underlying mechanisms are unknown. The novel treatment provided here depends on new evidence from DOX-treated H9c2 cells, which significantly enhanced insulin-like growth factor (IGF) II receptor (IGF-IIR) pathways that activated calcineurin and phosphorylated dynamin-related protein 1 (p-Drp1) at ser616 (p-Drp1[ser616]); cells undergo apoptosis due to these factors, which translocate to mitochondria and disrupt their function and integrity, and in terms of herbal medicine treatment, which significantly blocked these phenomena. Thus, our findings indicate that maintaining integrity of mitochondria is an essential element in lowering DOX-induced cytotoxicity, which further emphasizes that our herbal medicine can successfully block IGF-IIR pathways and could potentially act as an alternative mechanism in terms of cardioprotective against doxorubicin.

KEYWORDS
cardiac apoptosis, doxorubicin, H9c2 cells, IGF-IIR signaling pathway, mitochondrial damage, *Ohwia caudata*

1 | INTRODUCTION

Doxorubicin (DOX) is currently used as a chemotherapy medication over the world in treating diverse malignancies, including breast cancer, lymphomas, leukemias, and solid tumors.[1] However, while potentially an ideal chemotherapeutic drug, DOX administration has severe adverse effects, including extravasation, alopecia, vomiting, immunological suppression, and, most critically, cardiotoxicity.[2] Cardiomyocyte loss and cardiac dysfunction mainly happen because of the activation of apoptotic pathways, as well as myocardial infarction and heart failure, which are both caused by apoptosis.[3,4] During the initial phases, hypertrophy of the cardiac muscle has a positive effect, mainly on cardiac function by increasing the morphology of cardiomyocytes, which strengthens impulses in functional hypertrophy. Nevertheless, sustained stress promotes systolic disorder, which often contributes to chronic hypertrophy and cardiac arrest in the human body.

Chronic heart failure is caused by vascular remodeling of anatomical changes generated by numerous heart disorders, including chronic hypertension, myocardial infarction, or toxic chemical exposure.[5] The role of mitochondrial imbalance in cell death caused by anticancer treatments is well recognized, and exposing cardiac cells to various cardiac diseases changes the activity of mitochondrial proteins. However, remodeling of the mitochondrial formation and mass accompanying the physiological modifications is less frequent. The drug-induced rapid increase of mitochondria dysfunction is frequently described in scientific journals, for example, following the therapy of cardiac injury.[6,7] Our study focuses on the relationship between apoptosis and alterations in the organization of mitochondrial mass.

The insulin-like growth factor II receptor (IGF-IIR) actuates myocardial fibrosis amid myocardial remodeling and promotes compulsive muscle expansion.[8,9] Moreover, some research groups found that DOX treatment induces cardiomyocyte apoptosis, drives IGF-IIR accumulation, and activates subsequent apoptotic pathway.[10] IGF-IIR expression is suppressed by the calcium iron channel under regular conditions. According to evidence, cardiovascular disease (CVD) is among the most common illnesses among different groups of people.[11,12] Furthermore, it has been demonstrated that estrogen-induced elevation of the IGF-IIR signaling pathways, particularly estrogen receptors, restrict cardiotoxicity through multiple mechanisms, such as JNK1/AKT/p-AKT and calcineurin/NF-AT3 pathway.[13–15] Our previous study revealed that the

cardioprotective impact via the estrogenic action of some Chinese herbs hinders IGF-IIR expression from securing cardiomyocytes.[16–18]

DOX cardiotoxicity is directly associated to mitochondrial injury, which is defined by a rapid decrease of mitochondrial membrane potential after dysregulation of mitochondrial regulatory mechanisms.[19,20] Mitochondria continuously experience a combination of fission and fusion, particularly contributes to mitochondrial quality assurance, leading to cardiac damage. Several proteins regulate fusion, for example, mitofusin (MFN) 1 (MFN 1) and 2 (MFN 2) and optic atrophy 1 (OPA 1). However, fission is regulated by dynamin-related protein 1 (Drp1), mitochondrial fission factor (MFF), mitochondrial fission protein 1 (FIS1), and mitochondrial dynamics proteins (MiD) 49 (MiD49) and MiD51 kDA.[21–23] Mitochondrial fusion generally enables for the merging of various mitochondrial substances, reducing damage to proteins in the mitochondria and DNA. Fission, on the other hand, produces less split mitochondrial components, allowing mitochondria to spread across a cell. Furthermore, excessive separation promotes to heart injury under specific situations, including DOX therapy, pressure exhaustion, and ischemia.[24,25]

Ohwia caudata (OC) is a herb of the family Fabaceae. It is commonly referred to as *Desmodium caudatum* in the genus *Desmodium*, and is used to treat rheumatic spinal pain, loose bowels, icterohepatitis, and colds.[26] The chemical composition of OC includes flavonoids, triterpenoids, and alkaloids. The flavonoids in the OC demonstrated reactive oxygen species quenching and anti-amyloid beta accumulation experiments.[27] Nevertheless, study on OC's possible inhibitory effects on CVD still needs to be completed.

In this work, we attempted to identify possible recovery components for cardiac injuries from aqueous extracts of OC. We examined mechanisms whereby these herbal compounds attenuate DOX-induced cytotoxicity, revealing a novel role of IGF-IIR signals in the mitochondrial imbalance in cardiomyoblast H9c2 cell line.

2 | MATERIALS AND METHODS

2.1 | Reagents and antibodies

Unless otherwise specified, all analytical-grade reagents used in this work were provided by Sigma-Aldrich. Mature, healthy, and dry leaves of OC were offered by a traditional herbal medicine drug store in Hualien City, Taiwan. The following primary antibodies were used in this study: IGF-IIR (sc-14414), MNF1 (sc-166644), MNF2 (sc-100560), p-Drp1 (sc-271583), p-AKT (sc-514032), p-GATA-4 (sc-377543), GAPDH (sc-32233), calcineurin (610259) (BD Biosciences), Tom 20 (#42406), COX IV (#11967), PARP (#9542), and cleaved caspase 3 (#9664) (Cell Signaling Technology). All secondary antibodies were obtained from Santa Cruz Biotechnology.

2.2 | Preparation of the aqueous extract of OC

The OC herbs (50 g) were washed and processed to a smooth powdery substance. The powder was mixed with 500 mL of purified water and boiled until it was reduced to 50 mL. To remove any solid impurities, the mixture was centrifuged for 15 min at 4°C and 10,000 rpm. The residual material was removed by filtering the aqueous OC extract in the supernatant. The filtered extract was kept at −20°C for further use.

2.3 | Cell culture

H9c2 cardiomyoblasts were procured from the American Type Culture Collection (ATCC) and cultivated in Dulbecco's modified essential medium (DMEM) enriched with fetal bovine serum (10%) in 95% air/5% CO_2, penicillin (100 U/mL), glutamine (2 mM), pyruvate (1 mM), and streptomycin (100 μg/mL) in humidified air at 37°C. According to supplier guidelines, H9c2 cells were best passaged at 70%–80% confluence due to their ability to differentiate potential.

2.4 | Cell viability assay by MTT

To ascertain viability of cells, a colorimetric method using the conversion of tetrazolium dye to a blue formazan reagent was employed. H9c2 cardiomyoblast cells were cultivated in 96-well plates, exposed to varying doses of 0.1–1.5 μM DOX for 6 h, and subsequently, the media was substituted with 100 μL of 0.5 mg/mL MTT (3-(4,5-dimethylthiazol-2-yl)–2,5-diphenyltetrazolium-bromide), allowing for a further 4 h of incubation (37°C). The purple crystals of formazan were mixed using 100 μL of DMSO. A spectrophotometer was used to detect absorbance at 590 nm. The proportion of control viability was used to calculate cell viability.

2.5 | Western blot analysis

To extract total protein, H9c2 cardiomyoblast cells were lysed (30 min) in a cell lysis buffer containing Tris (50 mM),

pH 7.5, NaCl (0.5 M), glycerol (10%), β-mercaptoethanol (BME) (1 mM), ethylenediaminetetraacetic acid (EDTA) (1.0 mM), IGEPAL-630 (1%), and a proteinase inhibitor. The supernatants were analyzed using the Bradford assay. Proteins were separated by SDS-PAGE (8%–13.5%) and then shifted to polyvinylidene difluoride (PVDF) membranes (Millipore). After blocking nonspecific protein binding (1 h) in Tris-buffered saline Tween-20 (TBST) with skim milk (5%), primary antibodies (1:1000 dilution in TBST) were used to blot overnight at 4°C. Immobilon Western chemiluminescent horseradish peroxidase (HRP) substrate (Millipore) was used to detect protein signals after 1 h of incubation with HRP-conjugated secondary antibodies (1:4000 dilution in TBST). The Amager 2200 digital imaging equipment was used to assess the immunoblots.

2.6 | Immunofluorescence assay

After washing with PBS, the cells were fixed in paraformaldehyde (4%) for 30 min at room temperature and then permeabilized in Triton X-100 (0.1%) for 5 min at 4°C. Next, fortified bovine calf serum (10%) in PBS was used to block the cells for 30 min at room temperature. The primary antibody was then allowed to incubate at 4°C for 24 h. The cells were rinsed and incubated at room temperature for 1 h with secondary antibody (bright red fluorescent-conjugated Alexa Fluor 594 goat anti-rabbit IgG and bright green fluorescent-conjugated Alexa Fluor 488 goat anti-mouse IgG [A11001, Invitrogen]). After that the cells were washed with PBS and stained for 5 min with 4′,6-diamidino-2-phenylindole dihydrochloride (DAPI). An OLYMPUS BX53 microscope and an image analysis system were used to capture the images (Olympus Corporation).

2.7 | Analysis of mitochondria morphology

The mitochondrial morphology was assessed using Mito-Tracker Red (M7512, Invitrogen). All experimental protocols followed to the manufacturer's instructions. Photomicrographs were captured with an OLYMPUS BX53 microscope and image analysis system (Olympus Corporation).

2.8 | Determination of mitochondrial reactive oxygen species

Superoxide production in cell mitochondria was measured using MitoSOX (Invitrogen) molecular probes. Following 24 h of DOX exposure and OC treatment, the cells were subjected to treatment with MitoSOX for 30 min (37°C), then DAPI for 5 min to inspect the cell nucleus. Mitochondrial reactive oxygen species (ROS) production was evaluated by an OLYMPUS BX53 microscope equipped with an image analysis system (Olympus Corporation) at 510/580 nm for excitation and emission.

2.9 | TUNEL assay

According to the manufacturer's instructions, apoptotic cell death in H9c2 cells was identified by terminal deoxynucleotidyl transferase dUTP-mediated nick-end labeling (TUNEL) with an in situ cell death detection kit. The H9c2 cardiomyoblast cells were grown in eight-well Millicell EZ slides. The cells were permeabilized in Triton X-100 (0.1%) for 15 min following a 30-min fixation in PBS containing paraformaldehyde (4%). The slides were then incubated with the TUNEL reaction mixture at 37°C for 60 min in the dark in a humidified atmosphere. The nuclei were stained with DAPI (Sigma-Aldrich) at a concentration of 2 μg/mL for about 10 min. The staining patterns of DAPI (blue) and TUNEL-positive cells (green) were evaluated using a fluorescence microscope (Olympus).

2.10 | Flow cytometry assay

Flow cytometry analysis was carried out using the Annexin V-FITC/propidium iodide (PI) staining apoptosis detection kit (BD Biosciences). The cells underwent 6 h of treatment with DOX, 18 h of treatment with an OC extract, and two PBS washes. To examine apoptotic cells, BD Biosciences' FACS Canto system was employed.

2.11 | Measurement of cardiac hypertrophy

Initially, as was previously mentioned, the TUNEL assay experimental approach was employed. Subsequently, the cells were incubated using rhodamine-phalloidin (Invitrogen) for the purpose of identifying actin filaments, and the nucleus was stained using DAPI (Abcam). However, cell sizes were frequently amplified to 200× and inspected according to imaging system instructions. Cell surface area was analyzed using Image J software version 1.46.

2.12 | Statistical analysis

Data are shown as mean ± standard deviation (SD). The results were analyzed using one-way ANOVA. The Student's *t*-tests were used to compare the means of the

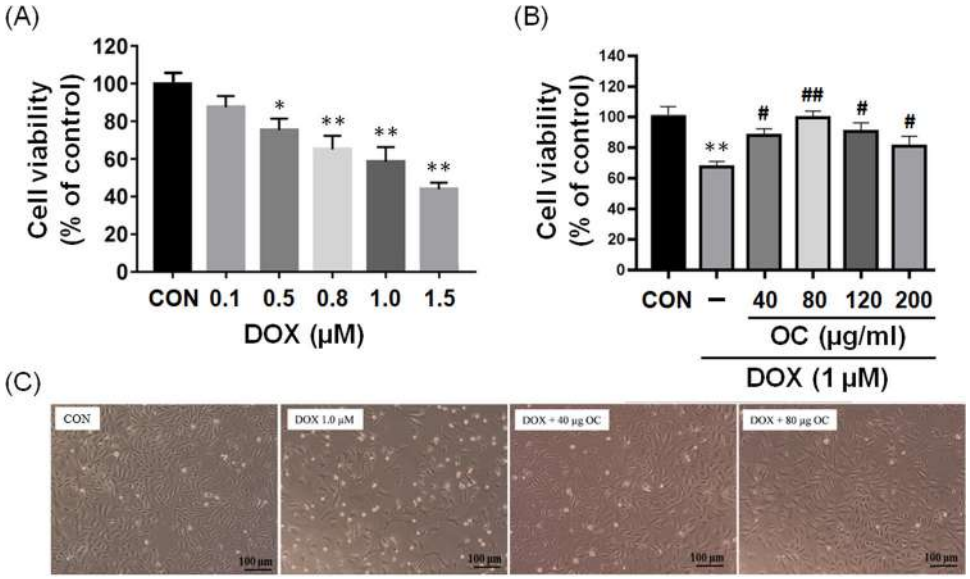

FIGURE 1 *Ohwia caudata* (OC) inhibits doxorubicin (DOX)-induced cytotoxicity in H9c2 cells. (A) The dose-dependent inhibition of DOX-induced cell viability in H9c2 cells. Cells received treatment with 0.1–1.5 μM DOX for 6 h. The cell viability was examined by MTT assay. (B) OC effectively rescues DOX-induced cytotoxicity in H9c2 cells. Cells received treatment with 1-μM DOX for 6 h, then washed with PBS and incubated with increasing doses of OC (40, 80, 120, and 200 μg/mL) for 18 h. The cell viability was then measured using the MTT assay. (C) The structure of cells after 6 h of treatment with 1 μM DOX, morphological changes in H9c2 cells were seen using a phase contrast microscope. Data are representative of at least three independent experiments. The values are presented as mean ± SD. $^{*}p < 0.05$, $^{**}p < 0.01$ indicate significant differences from the control group. $^{\#}p < 0.05$, $^{\#\#}p < 0.01$ indicate significant differences compared with DOX (1 μM)-treated group.

two groups. A *p*-value of less than 0.05 was considered statistically significant.

3 | RESULTS

3.1 | *O. caudata* inhibits doxorubicin-induced cytotoxicity in H9c2 cells

To assess DOX's cytotoxicity on H9c2 cells, we employed an MTT cell viability experiment. The results showed that DOX administration significantly reduced the proliferation of H9c2 cells in a dose (0.1–1.5 M)-dependent manner (Figure 1A). Furthermore, the efficacy of OC to prevent DOX-induced cytotoxicity was investigated. Our results showed that OC treatment (40–80 μg/mL) dose-dependently inhibited 1 μM DOX-induced cell death in H9c2 cells (Figure 1B). These findings reveal that the OC confers dose-dependent protection against DOX-induced cell death in H9c2 cells. Furthermore, the study revealed that the most efficient treatment concentration was 40−80 μg/mL OC; hence, H9c2 cardiomyoblast cells were used in the following tests with 40−80 μg/mL OC. Under phase contrast microscopy, we noticed that DOX (1 μM) treatment group cells were damaged due to the influence of the drugs compared to the control group, while OC treatment (40−80 μg/mL) recovered DOX-induced cardiomyoblast cell death significantly (Figure 1C).

3.2 | *O. caudata* inhibits doxorubicin-induced cardiotoxicity by regulating mitochondrial fission and fusion in H9c2 cells

We investigated the parameters that influence mitochondrial dynamics in our study. As expected, DOX did not increase mitochondrial fission or fusion (MNF1 and MNF2) protein levels. However, OC extracts boosted DOX-induced mitochondrial fission and fusion protein expression. Notably, in H9c2 cells, p-DRP1 (Ser616) expression increased, whereas p-DRP (Ser637) expression decreased in response to DOX (Figure 2A,B). Nevertheless, OC extracts enhanced the expression of p-DRP (Ser637) against DOX challenge H9c2 cells. The fluorescence intensities of MitoTracker Red were used to assess mitochondrial localization. In addition, immunofluorescence staining revealed that H9c2 cells downregulated p-Drp1 Ser616 from the cytoplasm to mitochondria, while OC inhibited protein expression (Figure 3A). Subsequently, MitoTracker Red with phosphorylated Drp1 Ser616

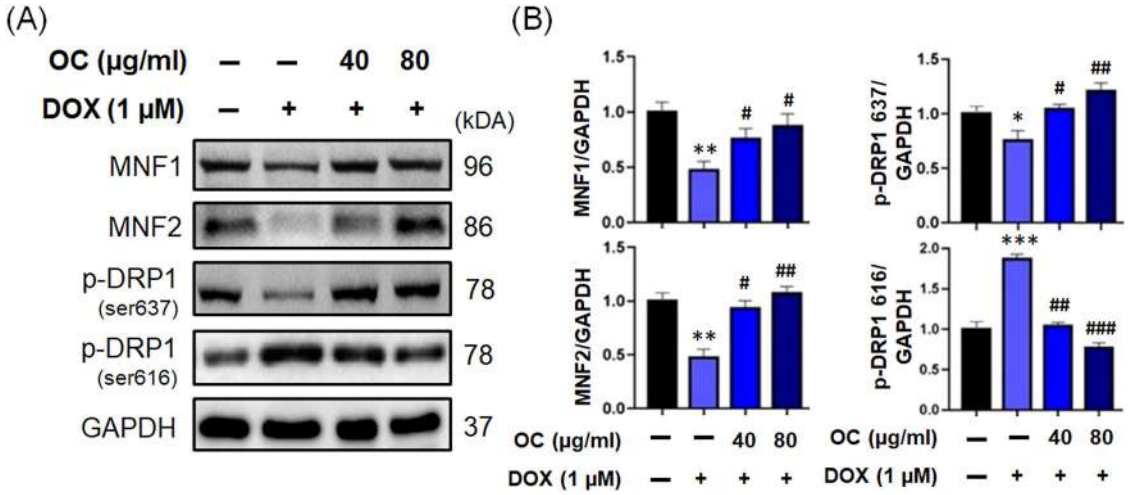

FIGURE 2 *Ohwia caudata* (OC) inhibits doxorubicin (DOX)-induced cardiotoxicity by regulating mitochondrial fission and fusion in H9c2 cells. (A) Cells received treatment with 1-μM DOX for 6 h, then washed with PBS and treated with 40 and 80 μg/mL of OC for 18 h. Western blot analysis was employed to determine the protein expression level of MNF1, MNF2, p-DRP1 (ser637), and p-DRP1 (ser616). The bars show the relative protein quantitation of MNF1, MNF2, p-DRP1 (ser637), and p-DRP1 (ser616). GAPDH served as an internal control. Data are representative of at least three independent experiments. The values are presented as mean ± SD. $^{*}p < 0.05$, $^{**}p < 0.01$, $^{***}p < 0.001$ indicate significant differences compared with control group. $^{\#}p < 0.05$, $^{\#\#}p < 0.01$, $^{\#\#\#}p < 0.001$ indicate significant differences compared with DOX (1 μM)-treated group.

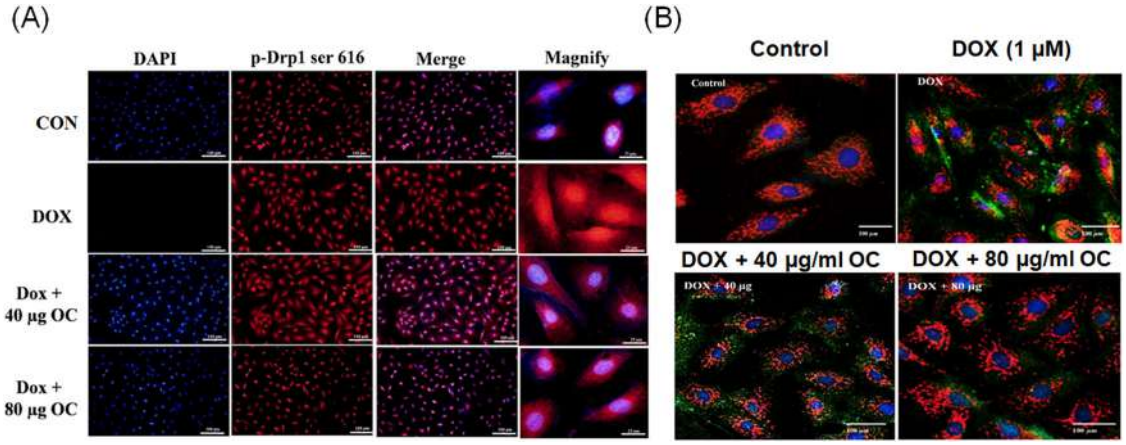

FIGURE 3 *Ohwia caudata* (OC) regulates phosphorylated Drp1 ser616 translocation and inhibits mitochondrial fission. (A) Cells received treatment with 1-μM DOX for 6 h, then washed with PBS and treated with 40 and 80 μg/mL of OC for 18 h. p-Drp1 ser616 expression (red) identified using immunofluorescence assay, and the mitochondria were labeled with MitoTracker Red. Nuclei were DAPI. Drp1 localizes to the cytoplasm and can trigger the serine phosphorylation-regulated pathway. Ser616 phosphorylation activates the mitochondrial fission site via DOX, resulting in mitochondrial fission and mitochondrial malfunction in H9c2 cells. However, OC inhibits this translocation site with increasing concentration. (B) OC suppresses p-Drp1 ser616 phosphorylation to prevent the mitochondrial fission induced by DOX in H9c2 cardiomyoblast cells by MitoTracker Red (scale bar = 100 μm).

staining results demonstrated that it could not traverse cytoplasm to mitochondria (Figure 3B). Phosphorylation ser637 is a translocated protein, and according to our data, the DOX group translocated into the nucleus, but OC at 40 and 80 μg/mL to cytoplasm (Figure 4A). Moreover, MitoTracker Red staining with phosphorylated Drp1 637 exhibited the same result (Figure 4B).

3.3 | *O. caudata* suppresses the production of mitochondrial reactive oxygen species by doxorubicin in H9c2 cells

Numerous studies have revealed that ROS implicated the cell death caused by DOX.[28] DOX generates ROS such as superoxide and peroxynitrite.[29] Therefore, in this

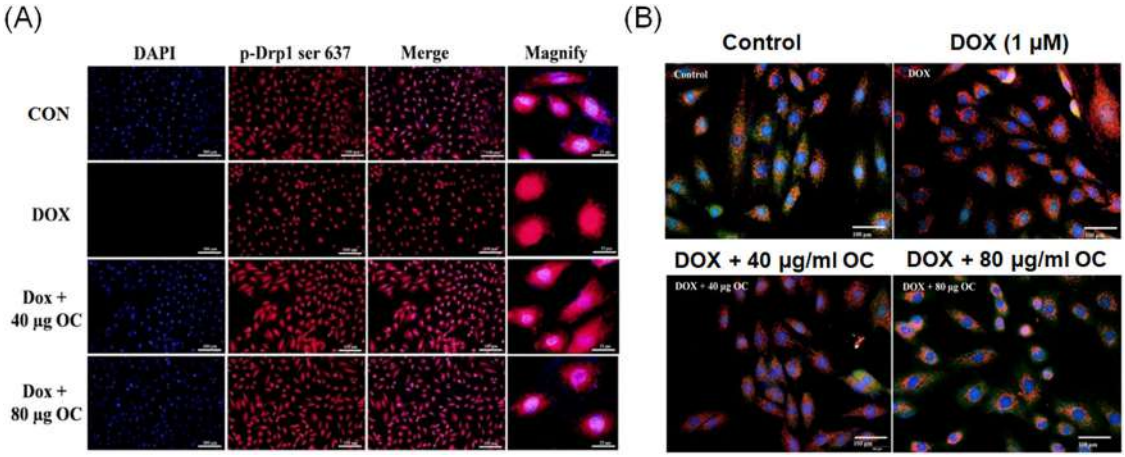

FIGURE 4 *Ohwia caudata* (OC) regulates phosphorylated Drp1 ser637 translocation and inhibits mitochondrial fusion. (A) Cells received treatment with 1-μM DOX for 6 h, then washed with PBS and treated with 40 and 80 μg/mL of OC for 18 h. p-Drp1 ser637 expression (red) identified using immunofluorescence assay and the mitochondria were stained with MitoTracker Red. Nuclei were stained with DAPI. Drp1 ser637 promoted Drp1 translocation from the cytosol to mitochondria and caused mitochondrial fusion by DOX. Thus, OC inhibits these translocation sites with a higher concentration. (B) OC inhibits p-Drp1 ser637 phosphorylation, which inhibits the mitochondrial fusion caused by DOX in H9c2 cells as detected by MitoTracker Red (scale bar = 100 μm).

investigation, we examined whether crude OC extract altered DOX's ROS production. Fluorescence microscopy was used to investigate H9c2 cells for mitochondrial superoxide production using the MitoSOX. Our data demonstrate that DOX enhanced mitochondrial superoxide production in comparison to untreated control cells. In contrast, OC treatment attenuated the intensity of DOX-induced MitoSOX fluorescence (Figure 5A,B). These findings imply that OC extract prevents DOX-induced cell death in H9c2 cells by decreasing the generation of mitochondrial ROS.

3.4 | *O. caudata* prevents doxorubicin-induced cardiotoxicity in H9c2 cells by regulating mitochondrial calcium homeostasis

Several recent investigations have demonstrated the biological significance of mitochondrial biogenesis.[29] To test our hypothesis, we attempted to correlate the expression of MCU, as we know that anti-MCU1 regulates mitochondrial calcium (Ca^{2+}) homeostasis and calcineurin mitochondrial biogenesis in H9c2 cells. Figure 6A,B reveals that DOX-induced calcineurin and anti-MCU1 expression levels were higher than those in the control group. OC extracts, on the other hand, suppressed DOX-induced calcineurin and anti-MCU1 expression at various dosages. Similarly, OC extracts inhibited DOX-induced COX IV expression at different doses. In contrast, at multiple dosages, OC extracts increase DOX-induced Tom20 expression (Figure 6A,B). These findings indicate that MCU mainly regulates mitochondrial biogenesis in H9c2 cells via modulating mitochondrial Ca^{2+} levels, while OC extracts substantially reduced protein expression.

3.5 | *O. caudata* suppresses cardiac apoptosis caused by doxorubicin by blocking the apoptotic IGF-IIR pathway in H9c2 cells

We have recently shown that elevated membrane-bound IGF-IIR causes caspase 3 and AKT-dependent cell death in response to heart failure damages, such as an abdominal aorta ligation-induced cardiovascular event or a spontaneous hypertension-induced event.[30] Therefore, our primary goal was to determine if IGF-IIR is involved in DOX-induced heart failure. When DOX doses are high, caspase 3 activation dramatically increases, resulting in apoptosis.[31] The IGF-IIR signals might mediate DOX-induced cardiomyoblast cell death, as IGF-IIR expression was significantly elevated. DOX administration dramatically increased the levels of cleaved caspase 3 and cleaved PARP in cells lacking IGF-IIR, suggesting that IGF-IIR was the cause of the DOX-induced cardiomyoblast cell death (Figure 7A,B).

On the other hand, OC extract may improve the cell's capacity to recover from apoptosis. After OC extracts were challenged with DOX, TUNEL + cardiomyoblasts were decreased, and as a result, their viability was also retained as usual (Figure 8A). Furthermore, flow cytometry data

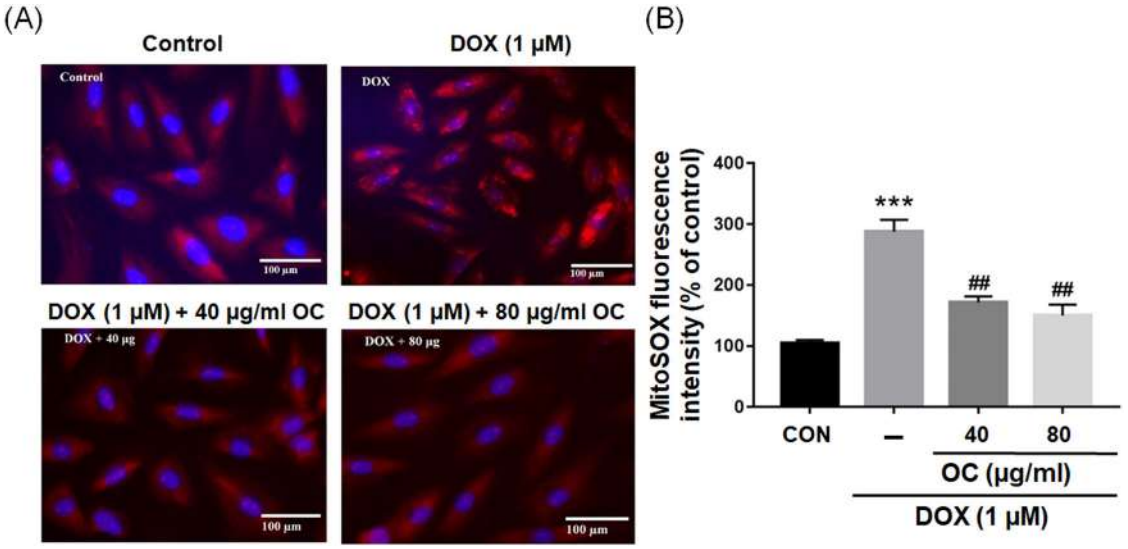

FIGURE 5 *Ohwia caudata* (OC) suppresses the production of mitochondrial reactive oxygen species (ROS) by doxorubicin (DOX) in H9c2 cells. (A) The MitoSOX Red reagent was employed to measure intracellular ROS. The production of intracellular ROS caused by DOX was investigated by treating H9c2 cells with 1 μM DOX for 6 h, followed by a PBS wash and incubation with 40 and 80 μg/mL concentrations of OC for 18 h. The intensity of ROS signals (red color) was detected using fluorescence imaging (scale bar = 100 μm). (B) The bars show the intensity of MitoSOX fluorescence. The treatment of H9c2 cells with 1-μM DOX increased intracellular ROS levels. However, OC treatment reduced DOX-induced ROS in H9c2 cells. Data are representative of at least three independent experiments. The values are presented as mean ± SD. $^{***}p < 0.001$ indicates significant differences compared with the control group. $^{\#\#}p < 0.01$ indicates significant differences compared with DOX (1 μM)-treated group.

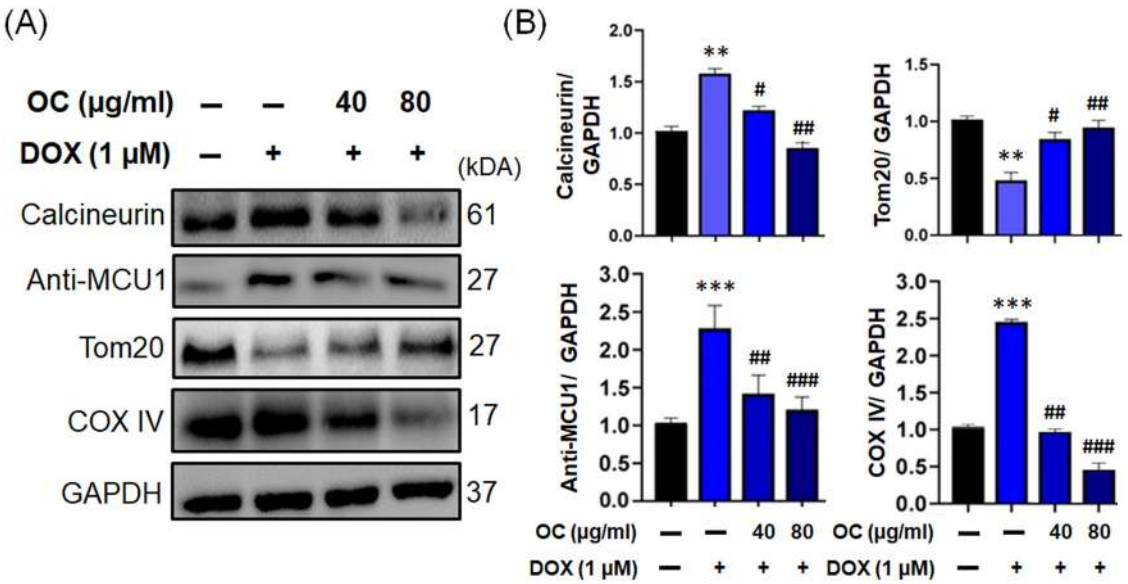

FIGURE 6 *Ohwia caudata* (OC) prevents doxorubicin (DOX)-induced cardiotoxicity in H9c2 cells by regulating mitochondrial calcium (Ca^{2+}) homeostasis. (A) Cells received treatment with 1-μM DOX for 6 h, then washed with PBS and treated with 40 and 80 μg/mL of OC for 18 h. Western blot analysis was used to evaluate the levels of the protein expression for calcineurin, anti-MCU1, Tom20, and COX IV. The bars show the relative protein quantitation of calcineurin, anti-MCU1, Tom20, and COX IV. GAPDH served as an Internal control. Data are representative of at least three independent experiments. The values are presented as mean ± SD. $^{**}p < 0.01$, $^{***}p < 0.001$ indicate significant differences compared with the control group. $^{\#}p < 0.05$, $^{\#\#}p < 0.01$, $^{\#\#\#}p < 0.001$ show significant differences compared with DOX (1 μM)-treated group.

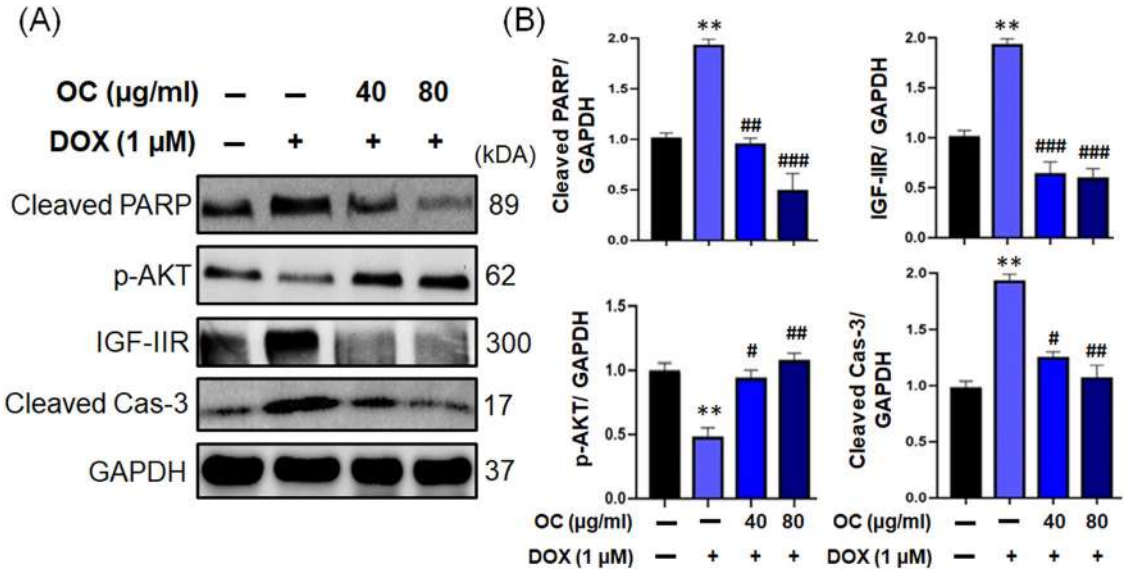

FIGURE 7 *Ohwia caudata* (OC) suppresses cardiac apoptosis caused by doxorubicin (DOX) by blocking the apoptotic IGF-IIR pathway in H9c2 cells. (A) Cells received treatment with 1-μM DOX for 6 h, then washed with PBS and treated with 40 and 80 μg/mL of OC for 18 h. Western blot analysis measured cleaved PARP, p-AKT, IGF-IIR, and cleaved caspase 3 protein expression level. The bars show the relative protein quantitation of cleaved PARP, p-AKT, IGF-IIR, and cleaved caspase 3. GAPDH served as an Internal control. Data are representative of at least three independent experiments. The values are presented as mean ± SD. $^{**}p < 0.01$ indicates significant differences from the control group. $^{\#}p < 0.05$, $^{\#\#}p < 0.01$, $^{\#\#\#}p < 0.001$ show significant differences compared with DOX (1 μM)-treated group.

indicated that both early and late apoptosis could be controlled marginally (Figure 8B). These data suggest that IGF-IIR-triggered apoptotic signaling pathways play an essential role in DOX-induced cardiomyoblast cell death, which OC extracts can significantly overcome.

3.6 | *O. caudata* mitigates doxorubicin-induced cardiac hypertrophy in H9c2 cells

Previous research showed that DOX can induce hypertrophy.[32] Therefore, DOX treatment was investigated to see whether it could directly cause cell hypertrophy and reactivate hypertrophic markers p-Gata-4 in H9c2 cardiomyoblast cells. The rhodamine-phalloidin stain demonstrated that DOX-treated cells had a higher surface area than untreated controls; nevertheless, different dosages of OC reduced surface area modestly (Figure 9A,B). Furthermore, Western blot demonstrated increased protein levels of p-Gata-4 in cells treated with DOX and a gradual decrease with OC extracts (Figure 9C,D). In addition, immunofluorescence staining showed that p-Gata-4 translocated into the nucleus (Figure 9E,F). Our findings revealed that OC extracts could diminish cardiac hypertrophy, which is speculated to be caused by the Gata-4 pathway.

4 | DISCUSSION

DOX has a broad range of anticancer properties and is frequently utilized.[2] Oxidative stress is the primary cause of heart damage due to cumulative dose-dependent effects. ROS and antioxidants are vital in reversing the redox imbalance that produces DOX-induced oxidative damage. Although oxidative stress has an impact in DOX-induced cardiotoxicity, preventive methods remain primarily ineffective. Several studies have described DOX-mediated cardiotoxicity therapy, which includes dexrazoxane or synthetic antioxidants, such as chemically generated antioxidants or natural plant extracts.[33,34] Most research focuses on the myocardium's mitochondria and endoplasmic reticulum. Previous research found that oxidative stress injury,[35] calcium excess,[36] and mitochondrial damage[37] are critical factors in DOX-induced cardiotoxicity. Accordingly, we need to develop new natural herbal medicine defensive agents that can counteract the detrimental effects of DOX.

OC, a traditional herbal medicine, is commonly employed in treating multiple disorders.[38,39] Its ingredients include alkaloids, triterpenoids, and flavonoids.[38,39] However, most studies concentrate on the organic extract rather than the medicinal qualities of the crude extract of OC, revealing a new area of inquiry for fundamental investigators to explore the potential medicinal

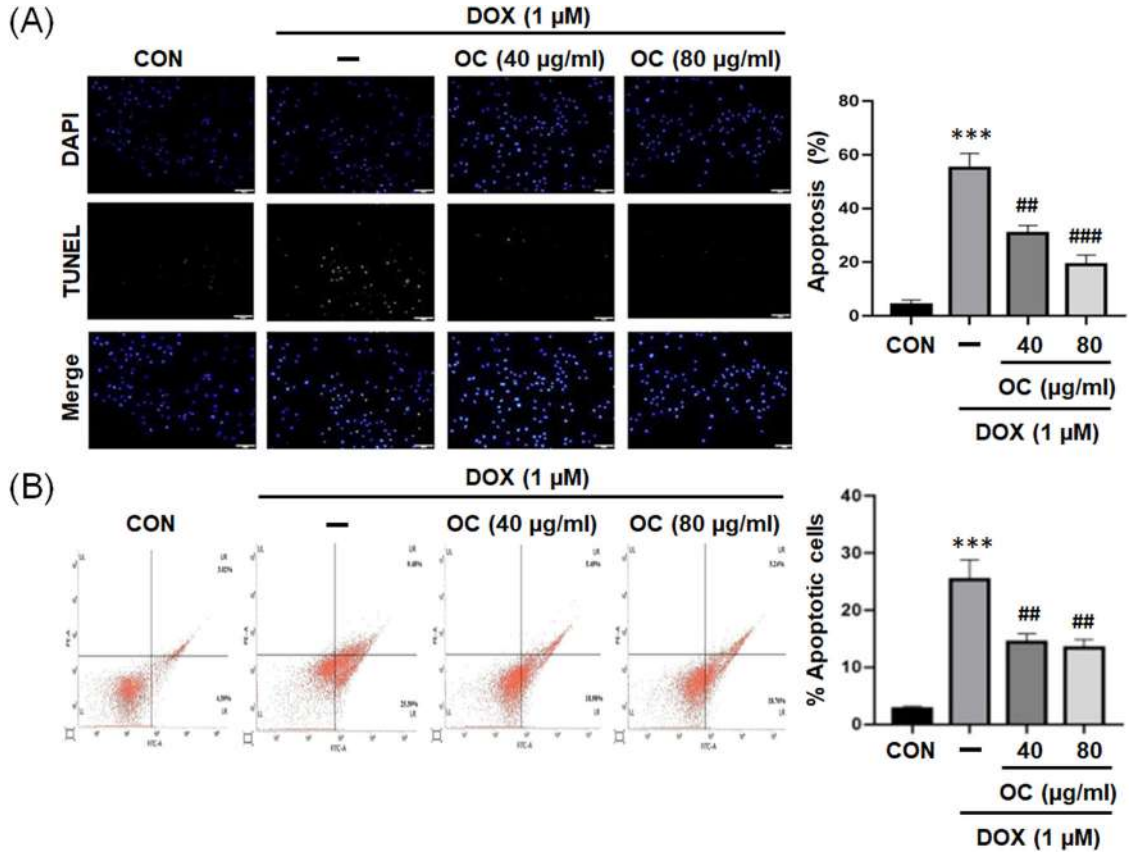

FIGURE 8 *Ohwia caudata* (OC) alleviates doxorubicin (DOX)-induced cardiac apoptosis in H9c2 cells. (A) Cells received treatment with 1-μM DOX for 6 h, then washed with PBS and treated with 40 and 80 μg/mL of OC for 18 h. The apoptotic cells were identified using the TUNEL assay (green), and the nuclei were counterstained with DAPI (blue) (scale bar = 10 μm). The bars show the percentage of TUNEL-positive apoptotic cells. Data are representative of at least three independent experiments. The values are presented as mean ± SD. ***$p < 0.001$ indicates significant differences compared with the control group. $^{\#\#}p < 0.01$, $^{\#\#\#}p < 0.001$ indicate significant differences compared with DOX (1 μM)-treated group. (B) Flow cytometry was used to examine cell apoptosis in H9c2 cells after stimulation with 1-μM DOX for 6 h, followed by washing with PBS and treatment with 40 and 80 μg/mL of OC for 18 h. OC significantly reduced cell apoptosis in DOX-challenged H9c2 cells. The bars show the percentage of apoptotic cells. Data are representative of at least three independent experiments. The values are presented as mean ± SD. ***$p < 0.001$ indicates significant differences compared with control group. $^{\#\#\#}p < 0.001$ shows significant differences compared with DOX (1 μM)-treated group.

properties of OC extract. The present study showed that herbal medicine OC extracts may have cardioprotective effects by promoting IGF-IIR deactivation and decreasing calcineurin/p-Drp1 (ser616) activity in DOX-induced cardiomyopathy and apoptosis. Data analysis revealed a consistent pattern of elevated ROS generation and pathological complications in heart function.

DOX-induced heart injury causes mitochondrial damage and impaired mitophagy.[40,41] DOX treatment in H9c2 cells elevated mitochondrial oxidative stress by dramatically increasing IGF-IIR overexpression. DOX treatment causes the cumulative accumulation of damaged proteins/organelles, which leads to the loss of antioxidant proteins and defective autophagy machinery, resulting in cell death and proteotoxicity. According to several reviews, natural herbal remedies derived from a vegetable in the *Allium* genus can decrease ROS production and protect from cardiac cell death.[42,43] Our results showed that OC extract treatment resulted in a dose-dependent reduction in ROS and p-Drp1 (ser616), calcineurin, and anti-MCU1 levels, as well as an increase in mitochondrial fusion proteins MNF1 and MNF2.

A recent study found that DOX administration induced apoptosis[44] via IGF-IIR signaling pathways. Our findings demonstrated that IGF-IIR, cleaved caspase 3, and cleaved PARP levels were decreased in response to a dose-dependent challenge of OC. OC aqueous extraction had similar effects on oxidative damage and cardiomyoblast apoptosis generated by DOX in H9C2 cardiomyoblast cells, which were comparable with the TUNEL assay and flow cytometry results. Mechanistically, we found that our crude extracts reduced DOX-induced cardiomyoblast death by inhibiting Drp1/caspase3/PARP signaling.

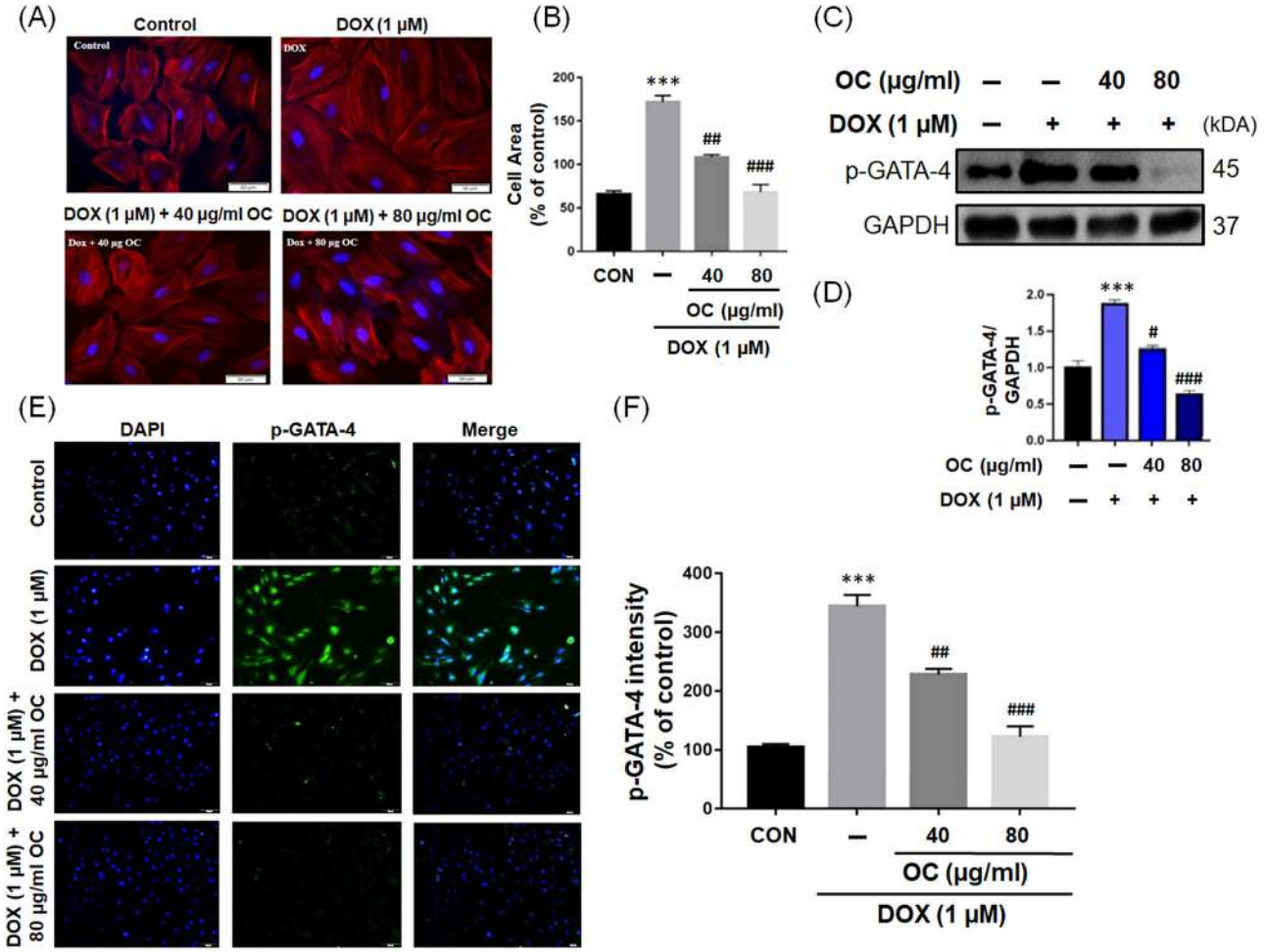

FIGURE 9 *Ohwia caudata* (OC) mitigates doxorubicin (DOX)-induced cardiac hypertrophy in H9c2 cells. (A) F-actin staining was used to evaluate cardiac hypertrophy in H9c2 cells (actin filaments are stained with Rhodamine-Phalloidin in red, while nuclei are labeled with DAPI in blue) after they were challenged with 1-μM DOX for 6 h, rinsed with PBS, then treated with 40 and 80 μg/mL of OC for 18 h. DOX treatment significantly increased cardiomyoblast size compared to the control group. OC-suppressed DOX-induced cell size increases in a dose-dependent manner (scale bar = 50 μm). (B) The bars show the quantitative analysis of cell area. Data are representative of at least three independent experiments. The values are presented as mean ± SD. ***$p < 0.001$ indicates significant differences compared with the control group. $^{\#\#}p < 0.01$, $^{\#\#\#}p < 0.001$ indicate significant differences compared with DOX (1 μM)-treated group. (C) Phosphorylated GATA-4 protein expression was determined by Western blot analysis. (D) The bars show the relative protein quantitation of p-Gata-4. GAPDH served as an Internal control. Data are representative of at least three independent experiments. The values are presented as mean ± SD. ***$p < 0.001$ indicates significant differences compared with the control group. $^{\#}p < 0.05$, $^{\#\#\#}p < 0.001$ show significant differences compared with DOX (1 μM)-treated group. (E) The immunofluorescence images of phosphorylated GATA-4 nuclear translocation acquired using fluorescence microscopy (magnification: 400×) are depicted. The nuclei were stained with DAPI (blue), while p-GATA-4 was labeled with Alexa Fluor 488 (green). (F) The bars show the intensity of p-GATA-4. Data are representative of at least three independent experiments. The values are presented as mean ± SD. ***$p < 0.001$ indicates significant differences compared with the control group. $^{\#\#}p < 0.01$, $^{\#\#\#}p < 0.001$ indicate significant differences compared with DOX (1 μM)-treated group.

Furthermore, we provided clear evidence that the IGF-IIR signaling pathways mediated the antioxidant action of aqueous OC extracts. We also showed that IGF-IIR was primarily responsible for activating the calcium channel calcineurin/Drp1. Based on the above findings, we propose that our aqueous OC extracts are a viable therapeutic agent against DOX-induced cardiotoxicity via IGF-IIR signaling pathways (Figure 10).

Cardiac hypertrophy is a frequent complication of hypertension that raises the possibility of coronary artery disease and other cardiac problems.[45] Extended cardiac hypertrophy increases the chance of heart failure, which leads to a higher risk of cardiovascular death.[46,47] However, there have been few cases of using natural herbal therapy to prevent heart hypertrophy. To the very best of our comprehension, this is the first study to explore the impact

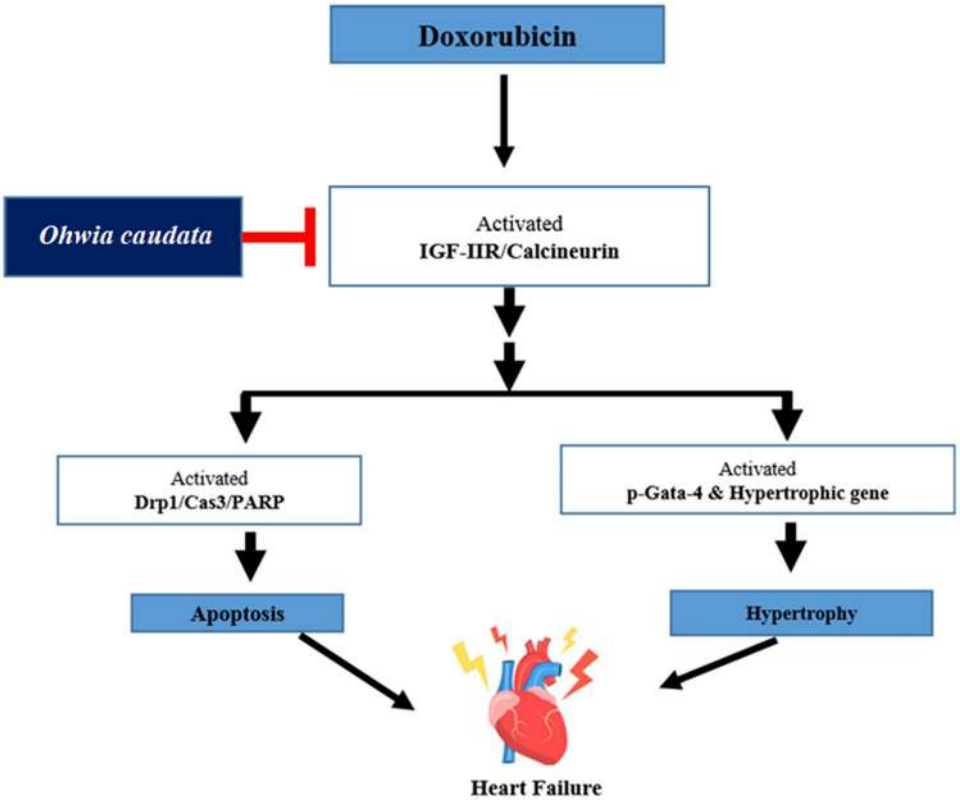

FIGURE 10 Schematic diagram depicting the preventive effects of *Ohwia caudata* on doxorubicin-induced cardiotoxicity by regulating mitochondrial dynamics via the IGF-IIR/p-Drp1/PARP signaling pathway.

of herbal therapy on heart injury. Hypertrophy of heart is defined by enhanced shape of cells and better synthesizing proteins via the transcriptional protein Gata-4.[2,48] The current study evaluated the preventive effect of natural medicine OC from DOX-induced cardiac hypertrophy in H9c2 cells. Cardiac hypertrophy is often caused by larger cells. Our results demonstrated that DOX administration increases cell size and shape in H9c2 cells, consistent with previous research. We examined the change in the cell's superficial area using F-actin staining. It is evident that DOX treatment increased cell surface region in H9c2 cells, whereas different doses of OC treatment reduced cell size. These findings support that OC can minimize cardiac hypertrophy by reducing DOX-induced cardiotoxicity. Furthermore, the calcineurin signaling pathway leads to the development of cardiac hypertrophy and advanced heart failure.

5 | CONCLUSION

Our study demonstrates that *O. caudata* extracts diminish DOX-induced cardiotoxicity in H9c2 cardiomyoblast cells by inhibiting the IGF-IIR/p-Drp1/PARP signaling pathway, which reduces oxidative stress, cardiac dysfunction, and apoptosis, and thus aids as a potential treatment target for preventing or alleviating DOX-induced cardiotoxicity. Nevertheless, further investigation is essential to determine the active ingredients in the *O. caudata* extract and to comprehend the mechanism of action.

AUTHOR CONTRIBUTIONS

Chien-Hao Wang, Chih-Yang Huang, and Wei-Wen Kuo: conceived and designed the study. Md. Nazmul Islam and Marthandam Asokan Shibu: performed experiments. Chia-Hua Kuo and Dennis Jine-Yuan Hsieh: collected samples. Pi-Yu Lin and Shinn-Zong Lin: performed the statistical data analysis. Md. Nazmul Islam and Samiraj Ramesh: wrote the manuscript. Samiraj Ramesh: professionally edited and thoroughly revised the manuscript. All authors read and approved the final version of the manuscript.

ACKNOWLEDGMENTS

This study was funded by Hualien Tzu Chi Hospital, Buddhist Tzu Chi Medical Foundation, Hualien, Taiwan (IMAR-109-01-04-01 and IMAR-112-01-02).

CONFLICT OF INTEREST STATEMENT

The authors declare that they have no conflicts of interest.

DATA AVAILABILITY STATEMENT

The data that support the findings of this study are available from the corresponding author upon reasonable request.

ORCID

Chih-Yang Huang https://orcid.org/0000-0003-2347-0411

REFERENCES

1. Cortes-Funes H, Coronado C. Role of anthracyclines in the era of targeted therapy. Cardiovasc Toxicol. 2007;7:56–60.
2. Octavia Y, Tocchetti CG, Gabrielson KL, Janssens S, Crijns HJ, Moens AL. Doxorubicin-induced cardiomyopathy: from molecular mechanisms to therapeutic strategies. J Mol Cell Cardiol. 2012;52:1213–25.
3. Liu SP, Shibu MA, Tsai FJ, Hsu YM, Tsai CH, Chung JG, et al. Tetramethylpyrazine reverses high-glucose induced hypoxic effects by negatively regulating HIF-1alpha induced BNIP3 expression to ameliorate H9c2 cardiomyoblast apoptosis. Nutr Metab (Lond). 2020;17:12.
4. Lin KH, Kuo WW, Jiang AZ, Pai P, Lin JY, Chen WK, et al. Tetramethylpyrazine ameliorated hypoxia-induced myocardial cell apoptosis via HIF-1alpha/JNK/p38 and IGFBP3/BNIP3 inhibition to upregulate PI3K/Akt survival signaling. Cell Physiol Biochem. 2015;36:334–44.
5. Azevedo PS, Polegato BF, Minicucci MF, Paiva SA, Zornoff LA. Cardiac remodeling: concepts, clinical impact, pathophysiological mechanisms and pharmacologic treatment. Arq Bras Cardiol. 2016;106:62–69.
6. Yang G, Song M, Hoang DH, Tran QH, Choe W, Kang I, et al. Melatonin prevents doxorubicin-induced cardiotoxicity through suppression of AMPKalpha2-dependent mitochondrial damage. Exp Mol Med. 2020;52:2055–68.
7. Hsieh Yuan, JD, Islam MN, Kuo WW, Shibu MA, Lai CH, et al. A combination of isoliquiritigenin with *Artemisia argyi* and *Ohwia caudata* water extracts attenuates oxidative stress, inflammation, and apoptosis by modulating Nrf2/Ho-1 signaling pathways in SD rats with doxorubicin-induced acute cardiotoxicity. Environ Toxicol. 2023;38:3026–42.
8. Chang MH, Kuo WW, Chen RJ, Lu MC, Tsai FJ, Kuo WH, et al. IGF-II/mannose 6-phosphate receptor activation induces metalloproteinase-9 matrix activity and increases plasminogen activator expression in H9c2 cardiomyoblast cells. J Mol Endocrinol. 2008;41:65–74.
9. Lin KH, Ramesh S, Agarwal S, Kuo WW, Kuo CH, Chen MY, et al. Fisetin attenuates doxorubicin-induced cardiotoxicity by inhibiting the insulin-like growth factor II receptor apoptotic pathway through estrogen receptor-alpha/-beta activation. Phytother Res. 2023;37:3964–81.
10. Huang PC, Kuo WW, Shen CY, Chen YF, Lin YM, Ho TJ, et al. Anthocyanin attenuates doxorubicin-induced cardiomyotoxicity via estrogen receptor-alpha/beta and stabilizes HSF1 to inhibit the IGF-IIR apoptotic pathway. Int J Mol Sci. 2016;17:1588.
11. Thompson J, Khalil RA. Gender differences in the regulation of vascular tone. Clin Exp Pharmacol Physiol. 2003;30:1–15. https://doi.org/10.1046/j.1440-1681.2003.03790.x
12. Chou SL, Ramesh S, Kuo CH, Ali A, Ho TJ, Chang KP, et al. Tanshinone IIA inhibits Leu27IGF-II-induced insulin-like growth factor receptor II signaling and myocardial apoptosis via estrogen receptor-mediated Akt activation. Environ Toxicol. 2022;37:142–50.
13. Donaldson C, Eder S, Baker C, Aronovitz MJ, Weiss AD, Hall-Porter M, et al. Estrogen attenuates left ventricular and cardiomyocyte hypertrophy by an estrogen receptor-dependent pathway that increases calcineurin degradation. Circ Res. 2009;104:265–75, 211p following 275.
14. Weng YS, Wang HF, Pai PY, Jong GP, Lai CH, Chung LC, et al. Tanshinone IIA prevents Leu27IGF-II-induced cardiomyocyte hypertrophy mediated by estrogen receptor and subsequent Akt activation. Am J Chin Med. 2015;43:1567–91.
15. Li CC, Ramesh S, Liu TY, Wang TF, Kuo WW, Kuo CH, et al. Overexpression of cardiac-specific IGF-IIRalpha accelerates the development of liver dysfunction through STZ-induced diabetic hepatocyte damage in transgenic rats. Environ Toxicol. 2022;37:2804–12.
16. Huang CY, Kuo WW, Kuo CH, Tsai FJ, Liu PY, Hsieh DJ. Protective effect of Danggui (Radix *Angelicae sinensis*) on angiotensin II-induced apoptosis in H9c2 cardiomyoblast cells. BMC Complement Altern Med. 2014;14:358.
17. Chang YM, Tsai CT, Wang CC, Chen YS, Lin YM, Kuo CH, et al. Alpinate oxyphyllae fructus (Alpinia oxyphylla Miq) extracts inhibit angiotensin-II induced cardiac apoptosis in H9c2 cardiomyoblast cells. Biosci Biotechnol Biochem. 2013;77:229–34.
18. Lin HJ, Ramesh S, Chang YM, Tsai CT, Tsai CC, Shibu MA, et al. D-galactose-induced toxicity associated senescence mitigated by alpinate oxyphyllae fructus fortified adipose-derived mesenchymal stem cells. Environ Toxicol. 2021;36:86–94.
19. Kim DS, Woo ER, Chae SW, Ha KC, Lee GH, Hong ST, et al. Plantainoside D protects adriamycin-induced apoptosis in H9c2 cardiac muscle cells via the inhibition of ROS generation and NF-kappaB activation. Life Sci. 2007;80:314–23.
20. Pereira GC, Silva AM, Diogo CV, Carvalho FS, Monteiro P, Oliveira PJ. Drug-induced cardiac mitochondrial toxicity and protection: from doxorubicin to carvedilol. Curr Pharm Des. 2011;17:2113–29.
21. Loson OC, Song Z, Chen H, Chan DC. Fis1, Mff, MiD49, and MiD51 mediate Drp1 recruitment in mitochondrial fission. Mol Biol Cell. 2013;24:659–67.
22. Atkins K, Dasgupta A, Chen KH, Mewburn J, Archer SL. The role of Drp1 adaptor proteins MiD49 and MiD51 in mitochondrial fission: implications for human disease. Clin Sci (Lond). 2016;130:1861–74.
23. Palmer CS, Elgass KD, Parton RG, Osellame LD, Stojanovski D, Ryan MT. Adaptor proteins MiD49 and MiD51 can act independently of Mff and Fis1 in Drp1 recruitment and are specific for mitochondrial fission. J Biol Chem. 2013;288:27584–93.
24. Sardao VA, Oliveira PJ, Holy J, Oliveira CR, Wallace KB. Morphological alterations induced by doxorubicin on H9c2 myoblasts: nuclear, mitochondrial, and cytoskeletal targets. Cell Biol Toxicol. 2009;25:227–43.
25. Gharanei M, Hussain A, Janneh O, Maddock H. Attenuation of doxorubicin-induced cardiotoxicity by mdivi-1: a mitochondrial division/mitophagy inhibitor. PLoS One. 2013;8:e77713.
26. Lee PY, Tsai BC, Sitorus MA, Lin PY, Lin SZ, Shih CY, et al. *Ohwia caudata* aqueous extract attenuates doxorubicin-

induced mitochondrial dysfunction in Wharton's jelly-derived mesenchymal stem cells. Environ Toxicol. 2023;38:2450–61.
27. Li W, Sun YN, Yan XT, Yang SY, Kim S, Chae D, et al. Anti-inflammatory and antioxidant activities of phenolic compounds from *Desmodium caudatum* leaves and stems. Arch Pharm Res. 2014;37:721–27.
28. Tsang WP, Chau SP, Kong SK, Fung KP, Kwok TT. Reactive oxygen species mediate doxorubicin induced p53-independent apoptosis. Life Sci. 2003;73:2047–58.
29. Mihm MJ, Yu F, Weinstein DM, Reiser PJ, Bauer JA. Intracellular distribution of peroxynitrite during doxorubicin cardiomyopathy: evidence for selective impairment of myofibrillar creatine kinase. Br J Pharmacol. 2002;135:581–88.
30. Lee SD, Chu CH, Huang EJ, Lu MC, Liu JY, Liu CJ, et al. Roles of insulin-like growth factor II in cardiomyoblast apoptosis and in hypertensive rat heart with abdominal aorta ligation. Am J Physiol Endocrinol Metab. 2006;291:E306–14.
31. Konorev EA, Vanamala S, Kalyanaraman B. Differences in doxorubicin-induced apoptotic signaling in adult and immature cardiomyocytes. Free Radic Biol Med. 2008;45:1723–28.
32. Chu CH, Tzang BS, Chen LM, Kuo CH, Cheng YC, Chen LY, et al. IGF-II/mannose-6-phosphate receptor signaling induced cell hypertrophy and atrial natriuretic peptide/BNP expression via Galphaq interaction and protein kinase C-alpha/CaMKII activation in H9c2 cardiomyoblast cells. J Endocrinol. 2008;197:381–90.
33. El-Agamy DS, El-Harbi KM, Khoshhal S, Ahmed N, Elkablawy MA, Shaaban AA, et al. Pristimerin protects against doxorubicin-induced cardiotoxicity and fibrosis through modulation of Nrf2 and MAPK/NF-kB signaling pathways. Cancer Manag Res. 2019;11:47–61.
34. Chen JY, He PC, Liu YH, Wei XB, Jiang L, Guo W, et al. Association of parenteral anticoagulation therapy with outcomes in chinese patients undergoing percutaneous coronary intervention for non-ST-segment elevation acute coronary syndrome. JAMA Intern Med. 2019;179:186–94.
35. Songbo M, Lang H, Xinyong C, Bin X, Ping Z, Liang S. Oxidative stress injury in doxorubicin-induced cardiotoxicity. Toxicol Lett. 2019;307:41–48.
36. Sag CM, Kohler AC, Anderson ME, Backs J, Maier LS. CaMKII-dependent SR Ca leak contributes to doxorubicin-induced impaired Ca handling in isolated cardiac myocytes. J Mol Cell Cardiol. 2011;51:749–59.
37. Jean SR, Tulumello DV, Riganti C, Liyanage SU, Schimmer AD, Kelley SO. Mitochondrial targeting of doxorubicin eliminates nuclear effects associated with cardiotoxicity. ACS Chem Biol. 2015;10:2007–15.
38. Kwon EB, Yang HJ, Choi JG, Li W. Protective effect of flavonoids from *Ohwia caudata* against influenza a virus infection. Molecules. 2020;25:4387.
39. Sun YW, Wang Y, Guo ZF, Du KC, Meng DL. Systems pharmacological approach to investigate the mechanism of *Ohwia caudata* for application to Alzheimer's disease. Molecules. 2019;24:1499.
40. Koleini N, Kardami E. Autophagy and mitophagy in the context of doxorubicin-induced cardiotoxicity. Oncotarget. 2017;8:46663–80.
41. Wang P, Wang L, Lu J, Hu Y, Wang Q, Li Z, et al. SESN2 protects against doxorubicin-induced cardiomyopathy via rescuing mitophagy and improving mitochondrial function. J Mol Cell Cardiol. 2019;133:125–37.
42. Kuo WW, Wang WJ, Tsai CY, Way CL, Hsu HH, Chen LM. Diallyl trisufide (DATS) suppresses high glucose-induced cardiomyocyte apoptosis by inhibiting JNK/NFkappaB signaling via attenuating ROS generation. Int J Cardiol. 2013;168:270–80.
43. Tsai CY, Wang CC, Lai TY, Tsu HN, Wang CH, Liang HY, et al. Antioxidant effects of diallyl trisulfide on high glucose-induced apoptosis are mediated by the PI3K/Akt-dependent activation of Nrf2 in cardiomyocytes. Int J Cardiol. 2013;168:1286–97.
44. Zhang X, Hu C, Kong CY, Song P, Wu HM, Xu SC, et al. FNDC5 alleviates oxidative stress and cardiomyocyte apoptosis in doxorubicin-induced cardiotoxicity via activating AKT. Cell Death Differ. 2020;27:540–55.
45. Oktay AA, Lavie CJ, Milani RV, Ventura HO, Gilliland YE, Shah S, et al. Current perspectives on left ventricular geometry in systemic hypertension. Prog Cardiovasc Dis. 2016;59:235–46.
46. Wang X, Zhang Y, Wang H, Zhao G, Fa X. MicroRNA-145 aggravates hypoxia-induced injury by targeting Rac1 in H9c2 cells. Cell Physiol Biochem. 2017;43:1974–86.
47. Zhang X, Zhang C, Wang N, Li Y, Zhang D, Li Q. MicroRNA-486 alleviates hypoxia-induced damage in H9c2 cells by targeting NDRG2 to inactivate JNK/C-Jun and NF-kappaB signaling pathways. Cell Physiol Biochem. 2018;48:2483–92.
48. Ferrans VJ, Clark JR, Zhang J, Yu ZX, Herman EH. Pathogenesis and prevention of doxorubicin cardiomyopathy. Tsitologiia. 1997;39:928–37.

How to cite this article: Chen J-K, Ramesh S, Islam MN, Shibu MA, Kuo C-H, Hsieh DJ-Y, et al. *Ohwia caudata* inhibits doxorubicin-induced cardiotoxicity by regulating mitochondrial dynamics via the IGF-IIR/p-Drp1/PARP signaling pathway. Biotechnol Appl Biochem. 2024;1–14. https://doi.org/10.1002/bab.2620